16th ICAAR
LISBOA 2020-2022

16th International Conference on
Alkali-Aggregate Reaction in Concrete
Lisboa | LNEC | Portugal | 31 May - 2 June 2022
http://icaar2020-2022.lnec.pt

Experimental study of the effects of mechanical restraints on ASR expansions in concrete

Joaquín Liaudat, Carlos M. López, Ignacio Carol

School of Civil Engineering of Barcelona (ETSECCPB)

Universitat Politècnica de Catalunya (UPC), Spain

joaquin.liaudat@upc.edu, carlos.maria.lopez@upc.edu, ignacio.carol.edu@upc.edu

Abstract

This paper summarizes an experimental campaign devoted to the study of the effect of (internal and external) mechanical restraints on Alkali-Silica Reaction (ASR) expansions in concrete made with soda-lime (SL) glass as reactive aggregate. The campaign included the development of two new experimental setups. The first setup made it possible to measure ASR expansion curves at the level of a single interface between a reactive aggregate and a cementitious matrix (mortar or cement paste). For this purpose, small sandwich-like specimens, with cement paste or mortar on top and bottom of a disc of SL glass in the middle, were used. These specimens were placed in airtight containers with a 1 m NaOH solution and heated in an oven at 60 °C. In these conditions, ASR products were formed rapidly at the glass-cement interfaces, inducing length changes in the specimen which were measured regularly. The interfaces developed expansions of about 30 μm before the SL glass got detached from the cementitious matrix. For the second experimental setup, a true-triaxial machine, specially designed for this purpose, was used to obtain ASR expansion curves of concrete cubical specimens subjected to three different triaxial stress states. The results obtained seem to confirm that: i) the volumetric ASR expansion rate is reduced as the applied volumetric compressive stress is increased, and ii) there is an increase of the expansion rate in the less compressed direction in detriment of the expansion rates in the most compressed ones. In both experiments, the formed ASR products were studied by means of SEM/EDS analyses.

Based on the results obtained in this study, as well as on published results from other authors, a reaction-expansion mechanism was proposed that might explain the effects of the stress state on the ASR expansions of concrete. This mechanism is based on the assumption that the gel water content of the ASR products is reduced as the applied compression stress is increased. Then, because the rate of formation of ASR products depends on the amount of (free and gel) pore water at the reaction site, the development of compression stresses in the ASR products filling a crack reduces the reaction rates at this location or even completely stops them.

Keywords: concrete; ASR; stress state; glass; interface

1. INTRODUCTION

Alkali-Silica Reaction (ASR) can be described as a particular type of chemical reaction in concrete involving the alkaline pore solution of the Hydrated Cement Paste (HCP) and various metastable forms of silica present in many natural and synthetic aggregate particles used in concrete [1, 2]. The silica structure is dissolved by the attack of hydroxyl anions, passing to the pore solution in aqueous forms which later recombine with calcium and alkali cations (always present in concrete pore solution) to form silicate hydrates of variable stoichiometric composition, the so-called 'ASR gel'. This reaction product is usually hygroscopic and swells as it absorbs water. The degree of hygroscopy and the associated volume change of the ASR gel depends mainly on its chemical composition and the Relative Humidity (RH) in the concrete pores. If the space available at the reaction site, i.e. pores, cracks, etc., is not enough to allocate the ASR gel, the 'swelling pressures produced by the gel induce the formation of microcracks close to the reaction sites, and these propagate and coalesce to produce cracking within the fabric of the concrete and overall expansion of the structural element affected' [3]. Since ASR was first identified in the late 1930s by T.E. Stanton [4, 5], extensive knowledge has been accumulated 'regarding the mechanisms of the reactions, the aggregate constituents that may react deleteriously, and precautions that can be taken to avoid resulting distress' [6]. However, the ASR expansion of concrete is a complex phenomenon and some aspects of it are still a matter of controversy. One of

these aspects is the influence of the stress state of concrete on the development of the ASR expansions, as well as the underlying mechanisms that determine this influence.

Since the early investigations, it was noticed that the stress state has an influence on the kinetics and distribution of ASR-induced cracking and expansions [7]. However, it was not until recent years that this topic became of particular interest for researchers and practitioners. This interest is motivated by the need of introducing the effect of the stress state in the numerical models used for the prediction of the evolution of the serviceability and strength of ASR-affected concrete structures. In the last 20 years a number of experimental studies on the effect of the stress state on ASR concrete expansions have been published [e.g. 8–13], but, nevertheless, the nature and magnitude of these effects, as well as the basic mechanisms behind them, have not been totally clarified.

In this context, a combined experimental-numerical study has been undertaken with the purpose of deepening in the understanding of the mechanisms by which the stress state affects the development of ASR concrete expansions. For the experimental part of the study, two new experimental setups have been developed and used in an extensive experimental campaign. The first one for studying ASR expansions at the level of a single aggregate-cementitious matrix (HCP or mortar) interface, and the second one for studying ASR expansions of concrete specimens under triaxial stress states. Based on the results obtained in the experimental study, as well as on published results from other authors, a reaction-expansion mechanism that may explain the effects of concrete stress state on ASR expansions is proposed. This paper focuses on this part of the study, summarizing the methodology and the results of the experimental campaign, which are more extensively described elsewhere [14–16].

In the second part of the study (not discussed here), the proposed reaction-expansion mechanism has been theoretically formulated and implemented in a coupled Chemo-Mechanical (C-M) Finite Element model, which has been used to demonstrate the ability of the proposed reaction-expansion mechanism to qualitative and/or qualitatively reproduce the experimental observations [14, 17].

2.   ASR INTERFACIAL EXPANSION TESTS

The aim of this test is to study ASR expansions at the level of single interface between a cementitious matrix and a reactive aggregate due to the formation of reaction products. Two types of cylindrical specimens of 33 mm diameter and 66 mm height are used. The first type, called 'reactive specimens' consists in sandwich-like specimens with a disc of reactive aggregate in the middle and cementitious matrix on top and bottom of it (Figure 2.1). The second type, called 'control specimens', consists in purely cementitious matrix specimens, without reactive aggregate. Steel gauge inserts are embedded at both ends of the specimens for measuring the length changes. The control specimens are used to evaluate the deformation of the cementitious matrix due to phenomena such as drying shrinkage or thermal expansions.
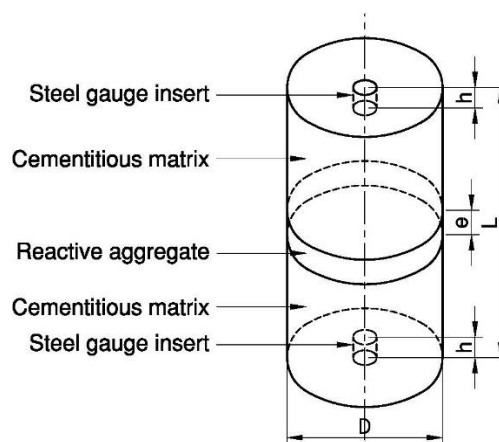

Figure 2.1: Scheme of a reactive specimen. Dimensions (in mm): D=33, L=66, h=5, e=6

The day after casting, the specimens are unmoulded and cured in airtight container with an alkaline solution at room temperature for 27 days. Then, the containers are heated in an oven at 60 ºC and kept at this temperature until the end of the test. During both stages, length changes of the specimens are measured regularly.

From the length change measurements of the active and the control specimens, the ASR expansion curves corresponding to a single matrix-aggregate interface are obtained using Equation (1), where L and ΔL are the length and the length change of the reactive specimen, respectively, e is the width of the reactive aggregate disc, h is the length of the steel gauge insert, $\bar{\varepsilon}$ is the average deformation of the control specimens, α_{agg} and α_{steel} are the thermal expansion coefficients of the aggregate and of the gauge insert steel, respectively, ΔT is the temperature variation from curing to exposure conditions, and d_I is the expansion at a single interface. For further details of the test method refer to [14, 16].

$$2d_I = \Delta L - \bar{\varepsilon}(L - 2h - e) - (e\alpha_{agg} + 2h\alpha_{steel})\Delta T \tag{1}$$

A typical set of interfacial expansion curves corresponding to specimens made soda-lime (SL) glass as reactive aggregate and mortar with siliceous sand as cementitious matrix is shown in Figure 2.2. When the curing stage is finished and the temperature is increased to 60 ºC, the specimens start to expand due to the formation of ASR products at the interfaces.
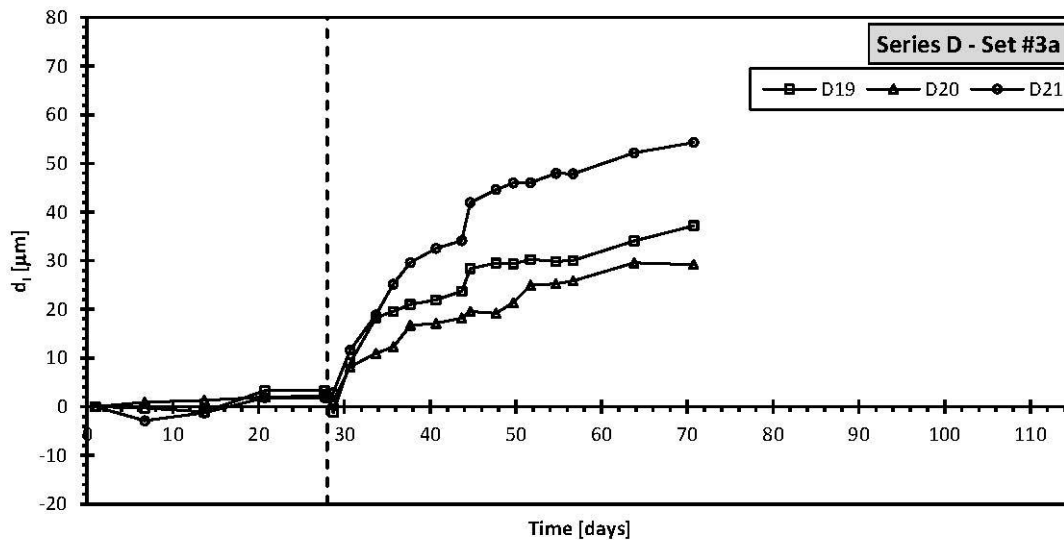

Figure 2.2: Interfacial expansion curves corresponding to specimens made with SL glass as reactive aggregate disc and mortar with siliceous sand as cementitious matrix. The dashed line indicates the end of curing stage (room temperature) and the beginning of exposure stage (60 ºC).

The reaction products at the interface are studied by means of SEM images and EDS microanalyses of polished sections of the specimens. For example, Figure 2.3 shows a set of images of the interfacial zone of a SL glass-cement paste specimen tested in the above-described conditions. In the left image, one can distinguish the glass at the upper part, the cement paste at the bottom part, and a layer in between which corresponds to reaction products. Note that the reaction products themselves are only visible at the limits of this layer, just besides the glass and the cement paste. The rest of the layer appears plain black due to the epoxy resin used in the preparation of the sample, which replace the reaction products that had been there but were lost in the cutting and polishing processes. The upper and bottom-right images, show in detail the different morphology of the reaction products located next to the glass and the cement paste, respectively. The normalized chemical composition of these reaction products obtained via EDS microanalyses is within the following ranges: Ca/Si = 1.00–1.50, (Na+K)/Si = 0.10–0.80.
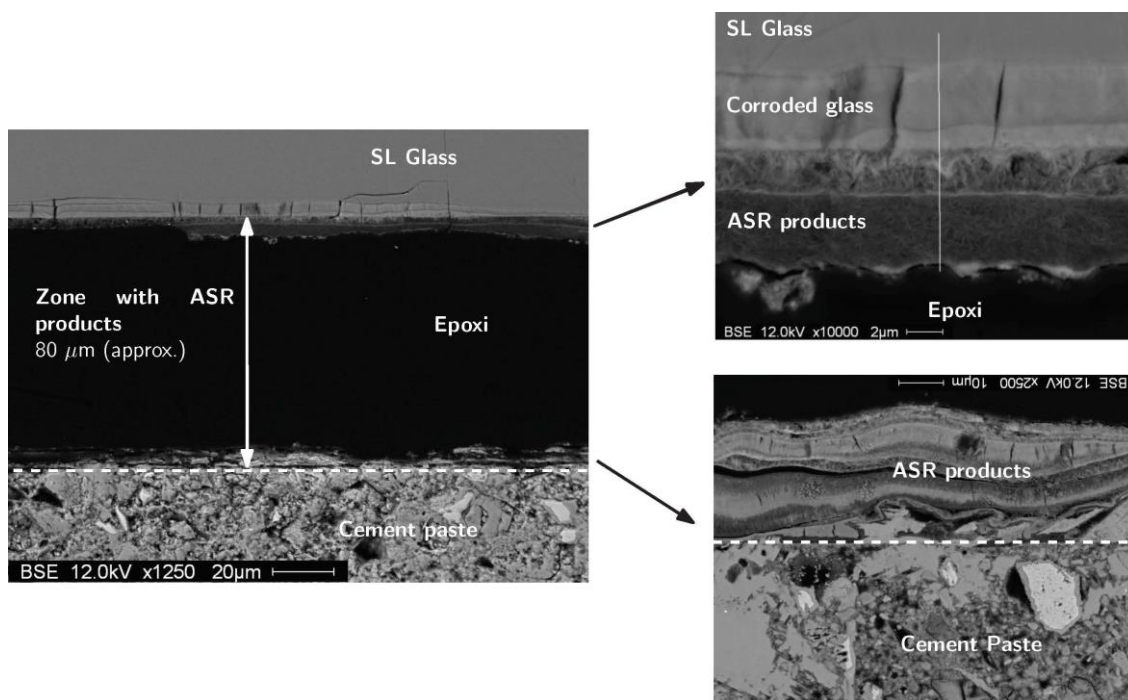
Figure 2.3: SEM images from the reacted zone interfacial zone of a specimen made with SL glass as reactive aggregate and cement paste as cementitious matrix [16].

In [14], additional results obtained with different cementitious matrices, reactive aggregates, and exposure conditions can be found, as well as detailed discussions of the effect of these factors. These results seem to indicate that:

- The ASR products formed in between SL glass and cement paste or mortar have relatively high calcium contents (molar Ca/Si = 1.0–1.5).
- The mass exchange of alkali and/or water between the specimens and the alkaline bath determines the kinetics of the interfacial expansions.
- The interfacial expansions are limited by the separation of the reactive aggregate (SL glass of Borosilicate glass) disc from the cementitious matrix occurring for interfacial expansions ranging between 30 µm and 50 µm.
- The type of cementitious matrix has an influence on the interfacial expansion rates. The fastest expansions were measured on specimens with matrix made of cement and Micro Silica (MS) paste, followed by the specimens made with plain cement paste, and the specimens made with mortar, in this order.

3. ASR CONFINED EXPANSION TESTS

The aim of this test is to measure ASR expansions in cubic concrete specimens under true triaxial confinement, i.e. under different constant stress in each principal direction. With this purpose, a testing machine, named 'Alkali-Aggregate Reaction Triaxial Machine' (AARTM), was originally designed and constructed by Prof. V.E. Saouma at University of Colorado-Boulder. The machine was later transferred to UPC (Barcelona), where a number of modification were introduced by the authors to the original design. See Figure 3.1 for general and detail views of the AARTM.
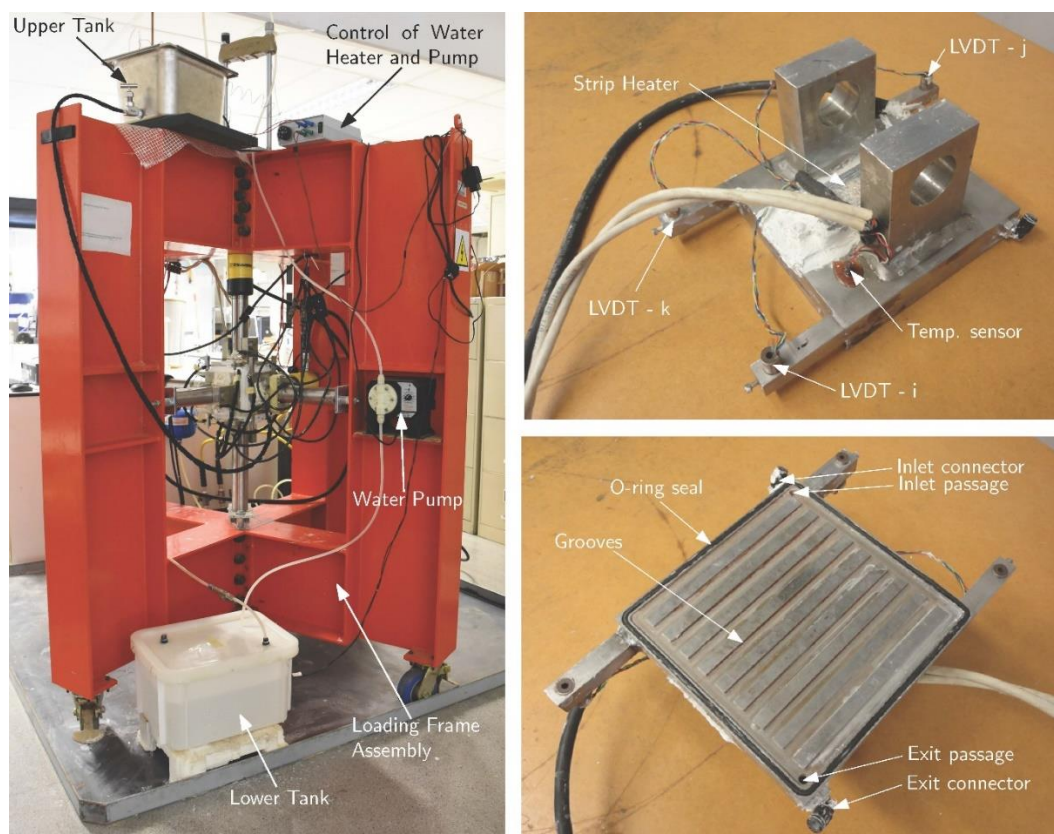
Figure 3.1: Left, general view of the AARTM. Right, detail views of an active loading plate of the AARTM [15].

The AARTM consists of a triaxial loading frame which can apply up to 9 MPa compression stress on each axis of a 150x150x150 mm cubical specimen. In contrast with other testing setups with triaxial confinement proposed in the literature [12, 18], the AARTM has the advantage of being capable of applying quasi-uniform constant true-triaxial stress states. The deformation of the specimen is measured with three displacement sensors (LVDTs) per axis, attached to the loading plates. The AARTM is capable of raising and maintaining the specimen temperature at a pre-set value between 30 and 70 ºC. In addition, the faces of the loading plates in contact with the specimen have carved grooves through which a solution may circulate to keep the specimen wet and supply alkalis. The confining pressure and the specimen temperature, as well as the data acquisition, are controlled by a LabVIEW-based computer system. For a more detailed description of the AARTM refer to [14, 15].

The AARTM has been used for a first experimental campaign in which two different kinds of concrete were tested. The first one, the 'control concrete', was made only with non-reactive aggregates. In contrast, the second one, the 'reactive concrete', was made with crushed SL glass as replacement of the coarser fraction of aggregates. Control and reactive specimens were tested in the same conditions with the purpose of isolating creep/shrinkage strains from ASR-induced expansions in the reactive specimens. Four different load cases were investigated: 0-0-0, 1-1-1, 9-9-1, and 9-9-9. This notation indicates the compression stress applied in each axis. For instance, '9-9-1' indicates that compression stresses of 9 MPa were applied in the X- and Y-direction and 1 MPa was applied in the Z-direction. The test temperature was 60 ºC and the circulating solution was 1 m NaOH solution. The load case 0-0-0 (free expansion) was not carried out with the AARTM because a minimum pressure is needed to prevent the leakage of the alkaline solution circulating in between the loading plates and the specimen. Alternatively, free expansion tests were performed with a different procedure, using airtight containers with alkaline solution for storing the specimens in an oven at 60 ºC, and extracting the specimens regularly to measure ASR expansions with a DEMEC strain gage. For additional information about the specimens preparation, curing conditions, and testing methodology refer to [14, 15].

Figure 3.2a—c show the axial strain curves of the reactive specimens tested with the AARTM, after deducting the creep strains obtained with control specimens in the same conditions (not presented here). For each load case, two specimens were tested, which are differentiated in the plots with circular

and square markers. Figure 3.2d shows the comparison of average volumetric strain curves, after deducting creep, obtained with the AARTM as well as with free expansion condtions.
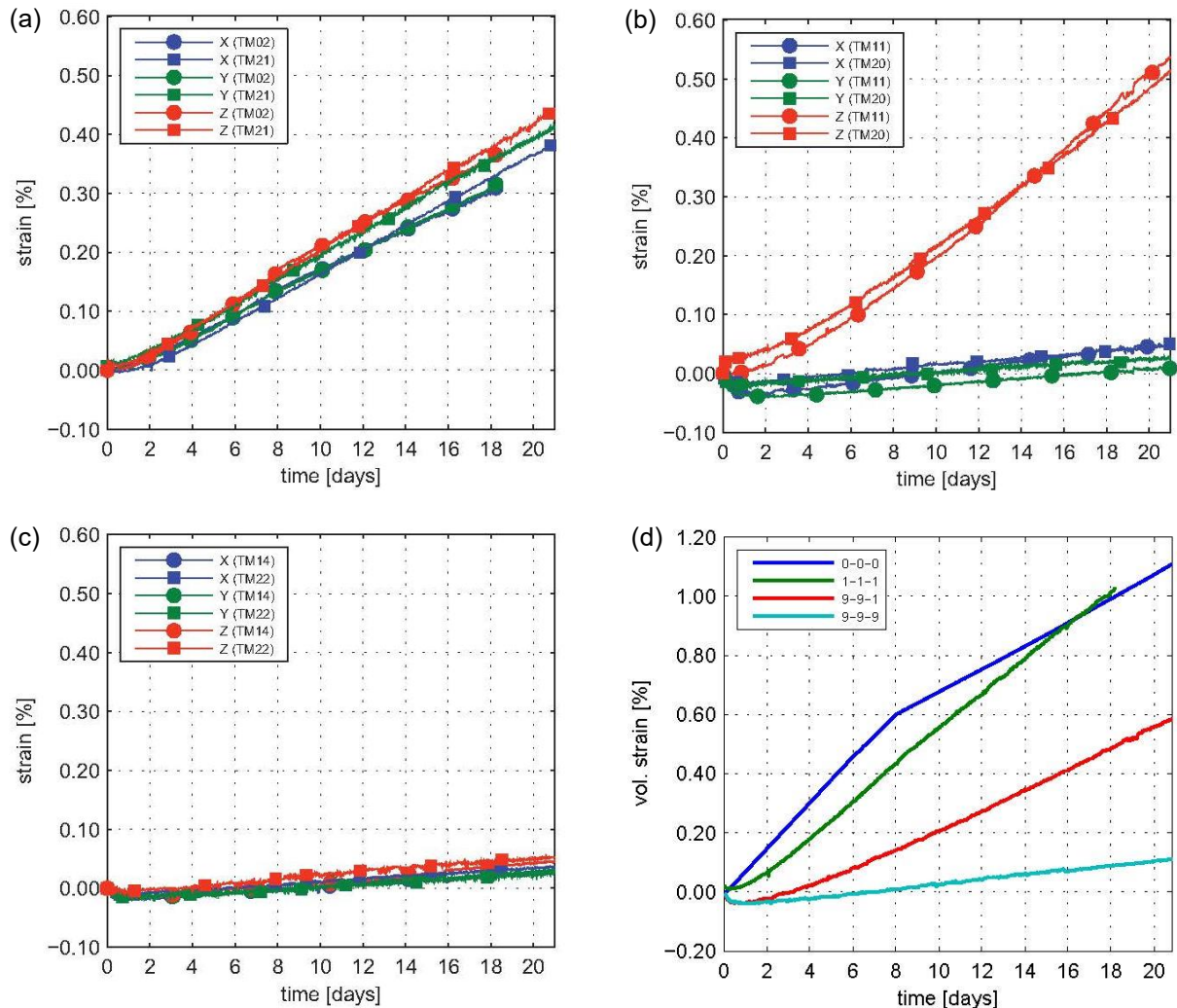

Figure 3.2: (a—c) Axial strain curves, after deducting creep, of reactive specimens under 1-1-1, 9-9-9, and 9-9-1 load cases, respectively. (d) Comparison of average volumetric strain curves, after deducting creep, of reactive specimens under different triaxial confinement stress values. After [15].

Let us first consider the ASR expansion curves obtained with the AARTM for isotropic load cases 1-1-1 (Figure 3.2a) and 9-9-9 (Figure 3.2c). As it was observed in the free expansion tests (not presented here), the expansion rates are roughly isotropic. The expansion rates under load case 1-1-1 are a little below than in free expansion conditions, but much higher than the expansion rates under load case 9-9-9. For load case 9-9-1 (Figure 3.2b), the expansion rates in the most loaded directions are similar to the expansion rates in the 9-9-9 load case, but, remarkably, the expansion rate in the Z-direction (the 1-MPa-direction) is higher than that measured for the 1-1-1 load case. This seems to indicate that there is a certain expansion transfer from the most compressed directions to the less compressed one. Finally, Figure 3.2d shows that the volumetric expansion rate decreases as the applied volumetric stress is increased.
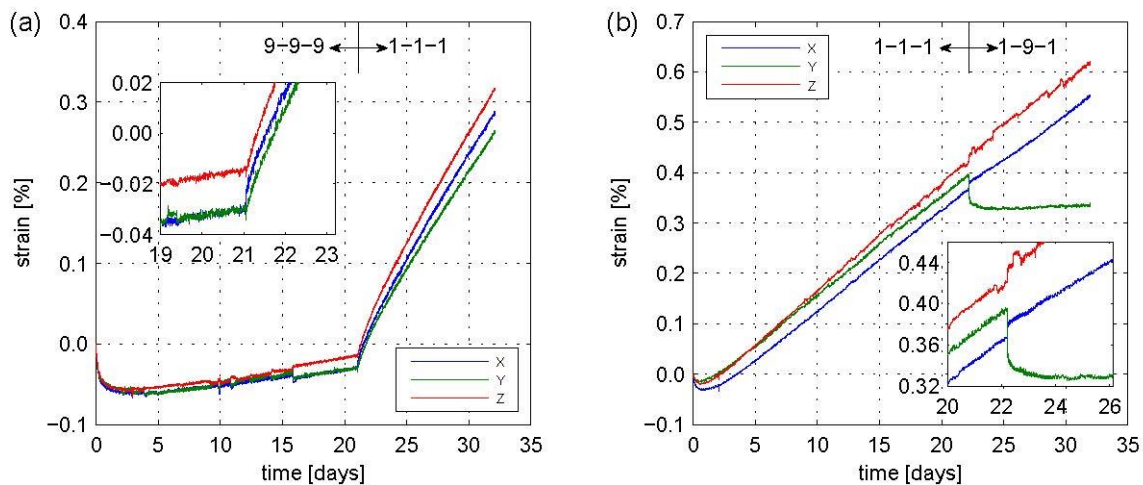
Figure 3.3: Axial strain curves (without deducting any creep effects) of: (a) reactive specimen first subjected to load case 9-9-9 for 21 days and then to load case 1-1-1 until the end of the test; (b) reactive specimen first subjected to load case 1-1-1 for 22 days and then to load case 1-9-1 until the end of the test. After [15].

After the standard testing time of 21 days had been completed, the stress states of two specimens (TM14 and TM21) were changed and the tests continued for an additional period of approximately 12 days. The axial strain curves of these specimens with the additional testing period are shown in Figure 3.3. These curves are the raw ones, i.e. without any creep deduction, because the counterpart control specimens were not subject to the same changes of the stress state.

The stresses on specimen TM14 were reduced from 9-9-9 to 1-1-1, resulting in a significant increase of the expansion rate, as it can be observed in Figure 3.3a. The expansion rates were maximum immediately after the stress change, decreasing asymptotically to constant rate values in the following days. Remarkably, no instantaneous elastic expansions due to the reduction of the compression stresses is distinguished in the curves. The asymptotic values of the expansion rates are about 30% greater than the ASR expansion rates obtained for load case 1-1-1 (Figure 3.2a). These greater expansion rates might be attributed to two different reasons:

- The decompression of the specimen may have originated a delayed elastic creep expansion of concrete, which could explain, at least in part, the initial variation of the expansion rates.
- The swelling of ASR gel formed under the 9-9-9 stress state due to water absorption when the confining stresses reduce to 1-1-1.

The stress state of specimen TM21 was changed after 22 days from 1-1-1 to 1-9-1 (Figure 3.3a). In contrast with the previous case, instantaneous strains are clearly distinguished: a negative strain jump in the Y-direction and smaller positive strain jumps in the X- and Z-directions (Poisson's effect). Subsequently, the expansion rate in the Y-direction goes practically to zero, while in the X- and Z-directions the expansions rates are 10–20% smaller than for the previous 1-1-1 stress state. Again, the net ASR expansion rates in the secondary load state cannot be obtained because of the lack of a counterpart control specimen with the same stress history. However, it may be expected that the deduction of the creep strains would result in a small increase of the expansion rate in the Y-direction and an even smaller, if any, reduction in the X- and Z-direction rates, due to Poisson's effect on creep strains. Therefore, the increase of the Y-stress seems not only to have reduced the expansion rate in the Y- direction, but also the expansion rates in the other two directions.

Clearly, additional research is needed to confirm the previous observations regarding the effect of changing the stress state on ASR expansions.

With the purpose of studying the ASR products formed, samples were taken from specimen TM02 (1-1-1 load case) for performing SEM/EDS analyses. Two of the SEM images obtained are shown in Figure 3.4. In those analyses, three types of ASR products have been identified:

- **Low-calcium product.** Mainly localized within cracks inside glass particles, with molar ratios Ca/Si≈0.22–0.35 and (Na+K)/Si≈0.14–0.28.

- **High-calcium product**. Localized within cracks in the limestone mortar, with molar ratios Ca/Si≈1.40–1.43 and (Na+K)/Si≈0.12–0.15.
- **Intermediate product.** Transitional product between the low- and high-calcium products, with calcium content ranging in between the two extreme values. Alkali content, in turn, tends to decrease with increasing calcium content.
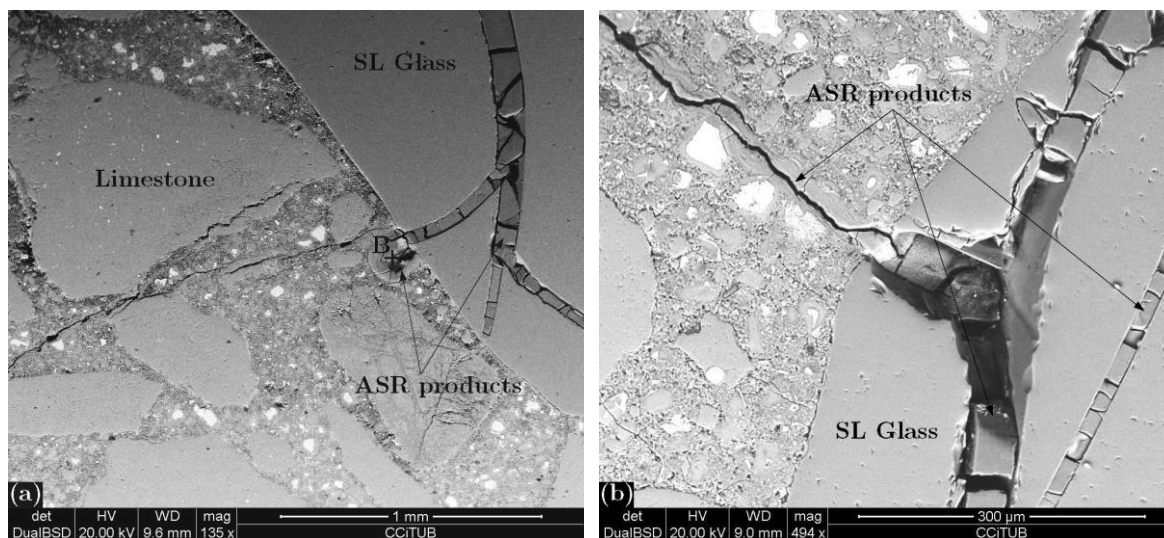

Figure 3.4: SEM images of a cross section of reactive specimen TM02 after testing (21 days under 1-1-1 load case) [16].

It is not possible to reconstruct the sequence of formation of the different ASR products and the propagation of cracks from a set of SEM images at a single testing time. However, based on the experimental study performed by Rajabipour et al. [19], it is possible to infer that ASR expansion begun mainly due to the precipitation of low-calcium products within pre-existing cracks inside glass particles. These pre-existing cracks are the residual result of the glass crushing process. The swelling of the low-calcium product within the residual cracks produced wedging stresses that propagate cracks towards the limestone mortar with the same orientation as the gel-filled residual cracks inside glass (Figure 3.4). The induced cracks in the limestone mortar were not initially filled with ASR products, but they were filled with intermediate and/or high-calcium products as the ASR progressed. Surprisingly, in most SEM images the glass-HCP interface appeared clean and did not show evidence of ASR products. In the few cases where a significant amount of ASR products was found at a glass-HCP interface, it was usually connected to a glass crack. Refer to [14] for additional SEM images and EDS analyses results.

4.   REACTION-EXPANSION MECHANISM FOR SL GLASS CONCRETE

In SL glass mortar specimens tested according to ASTM C1260 (free expansion in 1 M NaOH solution at 80 °C) [20], Rajabipour et al. [19] found a diffuse layer of high-calcium ASR product (Ca/Si = 1.34–1.51, Na/Si = 0.06–0.29) of about 20 µm at the boundary between the glass and the HCP. Rajabipour et al. referred to this product as 'Pozzolanic CSH', differentiating it from the products with lower calcium content (Ca/Si = 0.29–0.37, (Na+K)/Si = 0.38–0.42) formed within cracks in the glass particles, which were called 'ASR gel'. The Pozzolanic CSH was regarded by the authors as a non-expansive product, attributing the observed expansion of the mortar uniquely to the ASR gel. This distinction between calcium-rich products with low swelling capacity and calcium-poor products with high swelling capacity has been also made by other authors [e.g. 9, 21, 22].

The diffuse layer of Pozzolanic CSH described by Rajabipour et al. could not be identified in the samples taken from specimen TM02 after the Confined Expansion Test (Figure 3.4), since in most cases the contacts between the mortar and the glass particles appeared clean and did not show evidence of ASR products.

In any case, in both studies (the one by Rajabipour et al. [19] and ours) the amount/morphology/location of the ASR products formed at the glass-HCP interfaces of glass concrete or mortar, if any, substantially differ from the well differentiated layers of reaction products obtained with the Interfacial Expansion

Tests (Figure 2.4). Moreover, the interfacial expansion curves clearly indicate that high-calcium products (Pozzolanic CSH) is also capable of developing significant expansions.

A possible explanation to this incongruence may be found in the different mechanical restraint in each case. In the case of the Interfacial Expansion Tests, the ASR products only need to overcome the tensile strength of the glass-HCP interface in order to develop measurable expansions and to make room for further precipitation of reaction products. In contrast, in the case of glass particles within a cementitious matrix, the ASR products not only need to overcome the tensile strength of the glass-HCP interface, but also need to deform/crack the surrounding cementitious matrix (and even surpass superimposed external pressures, as in the case of specimen TM02). In other words, the swelling pressure needed for separating glass-HCP interfaces is certainly much lower in the first case than in the second case. These observations lead us to conjecture, in contrast with the interpretation of Rajabipour et al. [19], that the formation of high-calcium ASR products is indeed an expansive reaction, but an expansive reaction which can be slowed down by an applied pressure, or even inhibited if the applied pressure is higher than the Maximum Swelling-Pressure[1] (MSP) that can be developed by this reaction product. The low-calcium product within cracks inside glass particles, in turn, would have a similar behaviour but with a MSP significantly higher than the MSP of the high-calcium product. Considering that in the Confined Expansion Tests under load case 9-9-9, the glass concrete specimens were still capable of developing expansions, 9 MPa may be considered as a lower bound value of the MSP of low-calcium products. The real value has to be certainly higher, since, besides the external pressure, the low-calcium ASR products have also to overcome the internal restraints.

For the proposed interpretation of the experimental evidence, the ASR products are considered as an aggregation of colloidal particles of Calcium-Alkali-Silicate Hydrates (C–R–S–H) of variable composition which constitute a space-filling gel [1]. The C–R–S–H particles result from a number dissolution-formation reactions, in such a way that C–R–S–H with high calcium content is mainly formed at reaction sites close to HCP, while C–R–S–H with low calcium content is mainly formed in cracks inside the SL glass particles. In the resulting ASR products, two different fractions of water can be distinguished: the water chemically fixed in the C–R–S–H and the 'gel water', i.e. the water under the influence of absorbing forces. These forces may be attributed to different causes (e.g. osmotic pressure or double-layer repulsive forces) but, in any case, they are expected to be dependent on the chemical composition of the C–R–S–H. As water is absorbed, the content of gel water increases, the distance between the colloidal particles increases and, consequently, the 'bulk' volume of the ASR product increases. If this swelling is restrained by the solid skeleton around the reaction site, a mechanical pressure will build up on the ASR gel counteracting the absorption forces and, therefore, the volume of water absorbed will be lower than in free swelling conditions. In contrast, if the mechanical restraint is released, the original capacity of water absorption will be restored and the ASR products will absorb water and swell. The gel water is considered as part of the concrete pore solution, i.e. as an aqueous medium in which diffusion-reaction processes may take place. Therefore, a reduction of the gel water content is expected to reduce the ASR rate by locally reducing the volume of reacting medium, the 'wet' surface area of dissolving silica and/or the effective diffusion section.

5. CONCLUDING REMARKS

With regard to the Interfacial Expansion Tests, the proposed methodology meets the objective of measuring ASR expansions at the level of a single interface between a reactive aggregate and a cementitious matrix. This methodology can provide valuable information about the ASR expansion mechanisms, being at the same time inexpensive and easy to replicate. Moreover, the simplicity of the geometry and of the boundary conditions of the tested specimens make these tests ideal for the calibration of micro- and meso-scale numerical models for ASR expansion in concrete, as it has been done by the authors elsewhere [14, 17].

The results obtained demonstrate that the high-calcium ASR products (molar Ca/Si≈1.0–1.5) formed at the interfaces between SL glass and cement paste or mortar, which has been considered as non-expansive by some authors [19, 23], are actually capable of developing significant expansions at reaction sites with low mechanical restraint.

---

[1] Swelling pressure is defined as the pressure developed by the formation of ASR products under constant volume conditions.

With regard to the Confined Expansions Tests, the AARTM has shown to be capable of accurately applying and maintaining targeted true-triaxial compressive stress states and temperatures on the specimen, while keeping it in contact with a highly alkaline solution. In contrast with other testing setups with triaxial confinement proposed in the literature, the AARTM has the advantage of being capable of applying quasi-uniform constant true-triaxial stress states.

The results obtained with specimens made with crushed SL glass as reactive specimens seem to indicate that:

- The volumetric ASR expansion rate is reduced as the applied volumetric compressive stress is increased.
- Under anisotropic stress states, there is an increase of the expansion rate in the less compressed direction in detriment of the expansion rates in the most compressed directions.
- SEM/EDS analyses of the reaction products and cracking of a specimen tested under isotropic pressure of 1 MPa, indicate the presence of ASR products with variable calcium content, from low-calcium products (molar Ca/Si≈0.30) inside cracks within glass particles to high-calcium products (molar Ca/Si≈1.40) formed in contact with the HCP. Most of the ASR expansion and cracking is attributed to the low-calcium product.

Based on the experimental results obtained with both testing methodologies, as well as on other experimental results found in the literature, a new reaction-expansion mechanism for ASR in SL glass concrete has been proposed. This mechanism is based on the assumption that the gel water content of the ASR products is reduced as the applied compression stress is increased. Then, because the rate of formation of ASR products depends on the amount of (free and gel) pore water at the reaction site, the development of compression stresses in the ASR products filling a crack reduces the reaction rates at this location or even completely stops them. The proposed mechanism has been implemented in a coupled C-M FE model, which has been used to reproduce the experimental reproduce the experimental results summarized in this paper [14, 17].

6.　ACKNOWLEDGEMENTS

7.　REFERENCES

[1]　Rajabipour F, Giannini E, Dunant C, Ideker JH, Thomase MDA (2015) Alkali-silica reaction: Current understanding of the reaction mechanisms and the knowledge gaps. Cem Concr Res 76:130–146. https://doi.org/10.1016/j.cemconres.2015.05.024

[2]　Saouma VE, Xi Y (2004) CU/SA-XI-2004/001 Literature Review of Alkali Aggregate Reactions in Concrete Dams

[3]　Poole AB (1992) Introduction to alkali-aggregate reaction in concrete. In: Swamy RN (ed) The Alkali-Silica Reaction in Concrete. Blackie and Son Ltd., Glasgow, pp 1–29

[4]　Stanton T (1940) Expansion of concrete through reaction between cement and aggregate. In: Proceedings of American Society of Civil Engineers 66. pp 1781–1811

[5]　Stanton T, Porter O, Meder L, Nicol A (1942) California experience with the expansion of concrete through reaction between cement and aggregate. In: ACI Journal Proceedings. pp 209–236

[6]　ACI (1998) State-of-the-Art Report on Alkali-Aggregate Reactivity Reported by ACI Committee 221

[7]　McGowan JK, Vivian HE (1955) The Effect of Superincumbent Load on Mortar Bar Expansion. Aust J Appl Sci 6:94–99

[8]　Struble LJ, Diamond S (1981) Unstable swelling behaviour of alkali silica gels. Cem Concr Res 11:611–617

[9]   Leemann A (2012) Alkali-Silica Reaction autogenous deformations and pressure development in a model system. In: Drimalas T, Ideker JH, Fournier B (eds) 14th International Conference on Alkali-Aggregate Reactions in Concrete. Austin, Texas, USA

[10]   Dunant CF, Scrivener KL (2012) Effects of uniaxial stress on alkali-silica reaction induced expansion of concrete. Cem Concr Res 42:567–576. https://doi.org/10.1016/j.cemconres.2011.12.004

[11]   Larive C (1997) Apports combinés de l'expérimentation et de la modélisation à la compréhension de l'alcali-réaction et de ses effets mécaniques. École Nationale des Ponts et Chaussées, http://tel.archives-ouvertes.fr/tel-00520676/

[12]   Multon S, Toutlemonde F (2006) Effect of applied stresses on alkali-silica reaction-induced expansions. Cem Concr Res 36:912–920. https://doi.org/10.1016/j.cemconres.2005.11.012

[13]   Gautam BP, Panesar DK, Sheikh SA, Vecchio FJ (2017) Multiaxial Expansion-Stress Relationship for Alkali Silica Reaction-Affected Concrete. ACI Mater J 114:171–184. https://doi.org/10.14359/51689490

[14]   Liaudat J (2018) Experimental and numerical study of the effect of stress on ASR expansions in concrete. Universitat Politècnica de Catalunya, http://hdl.handle.net/10803/620624

[15]   Liaudat J, Carol I, López CM, Saouma VE (2018) ASR Expansions in Concrete under Triaxial Confinement. Cem Concr Compos 86:160–170. https://doi.org/10.1016/j.cemconcomp.2017.10.010

[16]   Liaudat J, Carol I, López CM, Leemann A (2019) ASR expansions at the level of a single glass-cement paste interface: experimental results and proposal of a reaction-expansion mechanism. Constr Build Mater 218:108–118. https://doi.org/10.1016/j.conbuildmat.2019.05.106

[17]   Liaudat J, Carol I, López CM (2020) Model for Alkali-Silica Reaction expansions in concrete using zero-thickness Chemo-Mechanical interface elements. Int J Solids Struct 207:145–177. https://doi.org/10.1016/j.ijsolstr.2020.09.019

[18]   Gautam BP, Panesar DK (2016) A new method of applying long-term multiaxial stresses in concrete specimens undergoing ASR, and their triaxial expansions. Mater Struct 49:3495–3508. https://doi.org/10.1617/s11527-015-0734-z

[19]   Rajabipour F, Maraghechi H, Fischer G (2010) Investigating the alkali-silica reaction of recycled glass aggregates in concrete materials. J Mater Civ Eng 22:1201–1208. https://doi.org/10.1061/(ASCE)MT.1943-5533.0000126

[20]   ASTM (2007) ASTM C1260-07 Standard Test Method for Potential Alkali Reactivity of Aggregate (Mortar-Bar Method). In: Annual Book of ASTM Standars. ASTM International

[21]   Leemann A, Le Saout G, Winnefeld F, et al (2011) Alkali-Silica Reaction: the influence of calcium on silica dissolution and the formation of reaction products. J Am Ceram Soc 94:1243–1249. https://doi.org/10.1111/j.1551-2916.2010.04202.x

[22]   Prezzi M, Monteiro PJM, Sposito G (1997) The alkali-silica reaction, Part I: use of the double-layer theory to explain the behavior of reaction-product gels. ACI Mater J 1:10–16

[23]   Maraghechi H, Shafaatian S-M-H, Fischer G, Rajabipour F (2012) The role of residual cracks on alkali silica reactivity of recycled glass aggregates. Cem Concr Res 34:41–47. https://doi.org/10.1016/j.cemconcomp.2011.07.004